Supplementary Information

Lewis-acid-engineered polymer electrolytes for all-solid-state lithium batteries

Sitong Yao,[a] Hongpeng Chen,[a] Su Yan,[a] Zehui Fan,[a] Lanhua Ma,[a] Luchen Jia[a] and Yunhua Xu*[a]

[a] School of Materials Science and Engineering, and State Key Laboratory of Advanced Materials for Intelligent Sensing, Tianjin University, Tianjin 300072, China

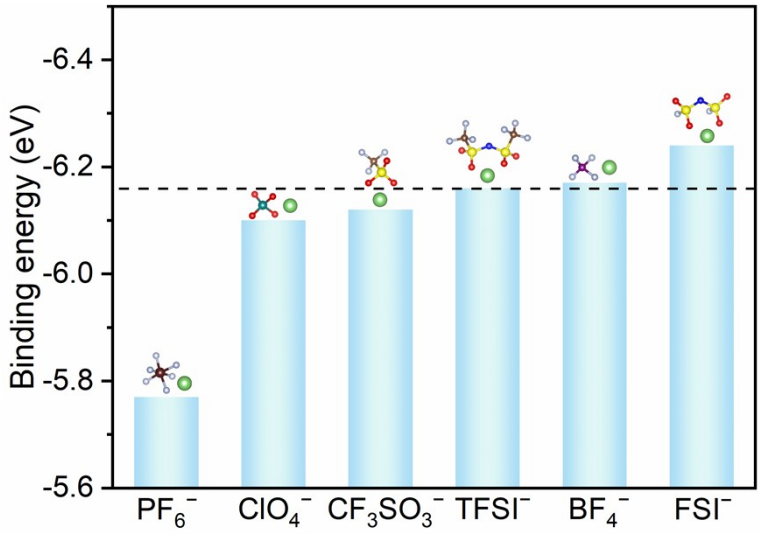

Fig. S1 Binding energies of various lithium salt anions with Li^+.

Fig. S2 Optical image of PEO/$Co(BF_4)_2$.

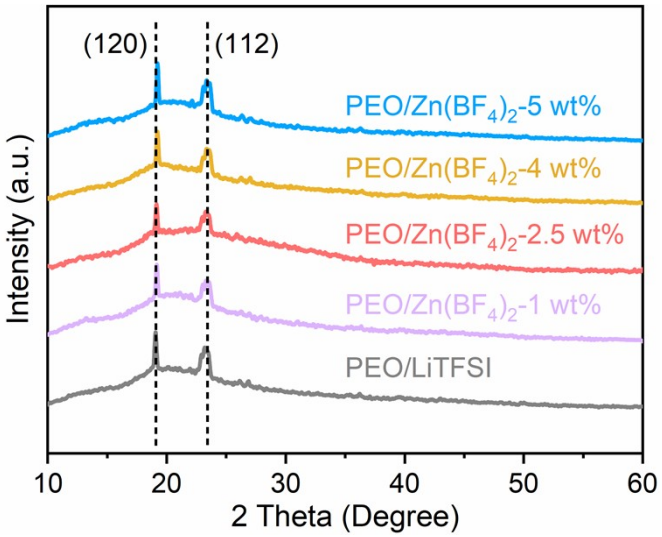

Fig. S3 XRD patterns of SPEs with various amounts of $Zn(BF_4)_2$.

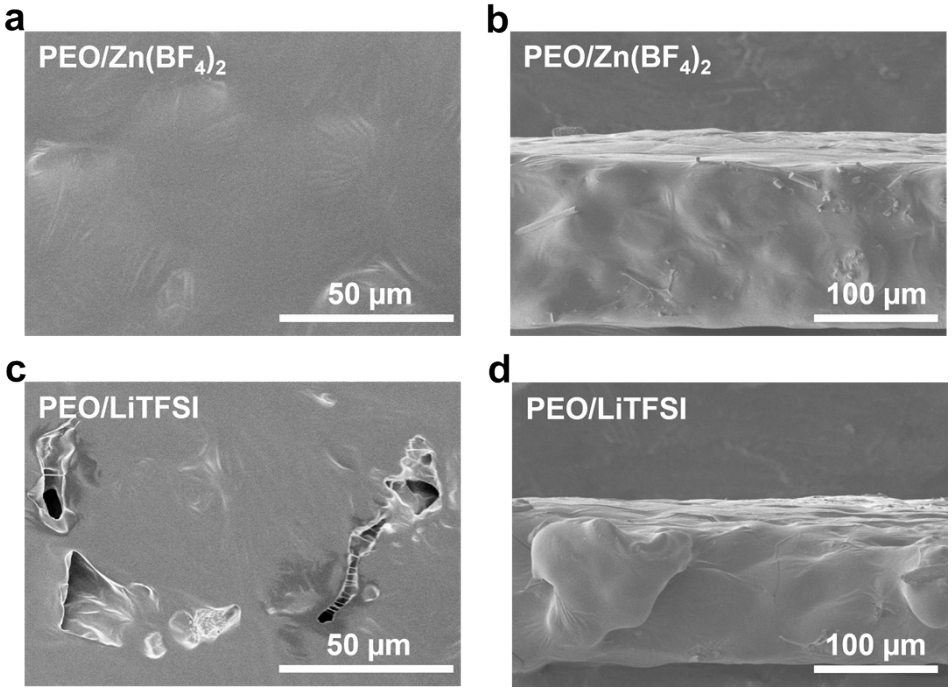

Fig. S4 Surface and cross-sectional SEM images of (a, b) $PEO/Zn(BF_4)_2$ and (c, d) PEO/LiTFSI.

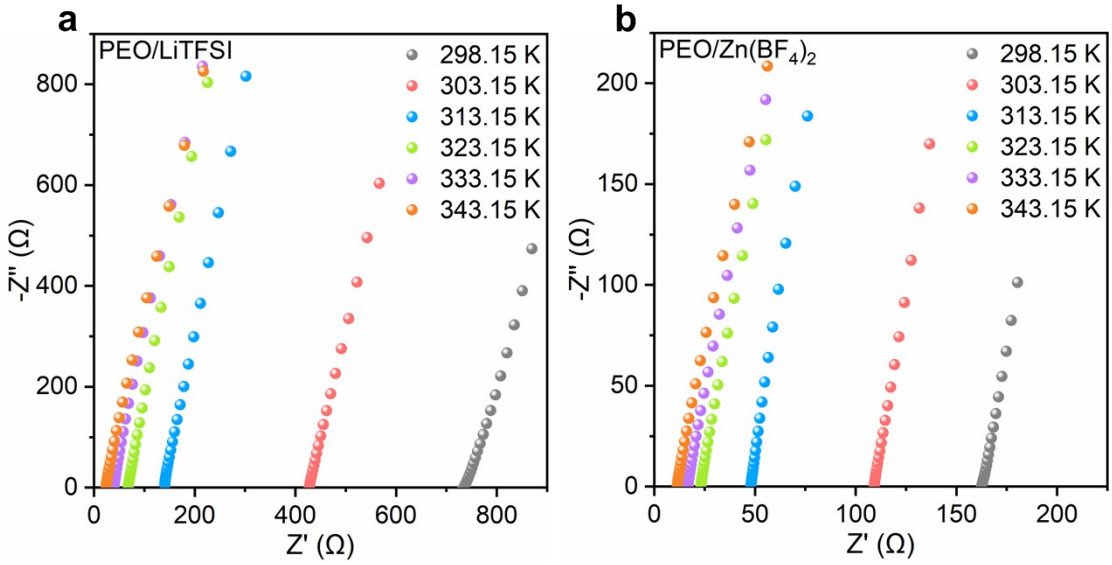

Fig. S5 EIS plots of the SS|SPE|SS symmetric cells with (a) PEO/LiTFSI and (b) PEO/$Zn(BF_4)_2$ at different temperatures ranging from 25 °C to 70 °C.

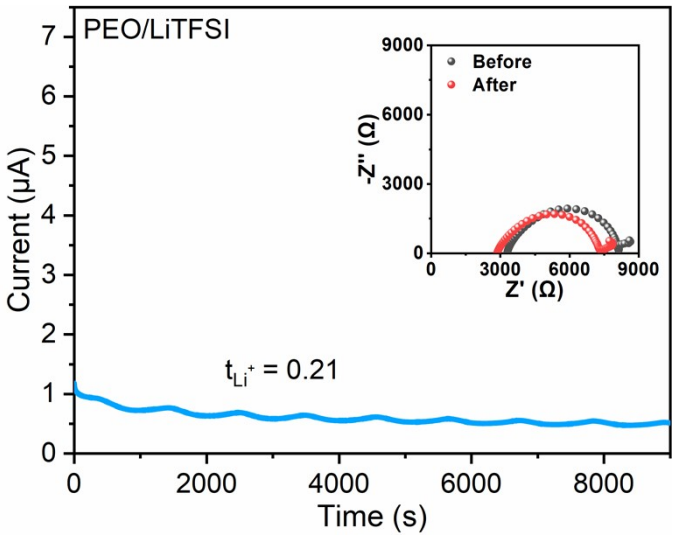

Fig. S6 Direct current polarization profile of the Li|PEO/LiTFSI|Li symmetric cell, inserting the EIS plots before and after polarization.

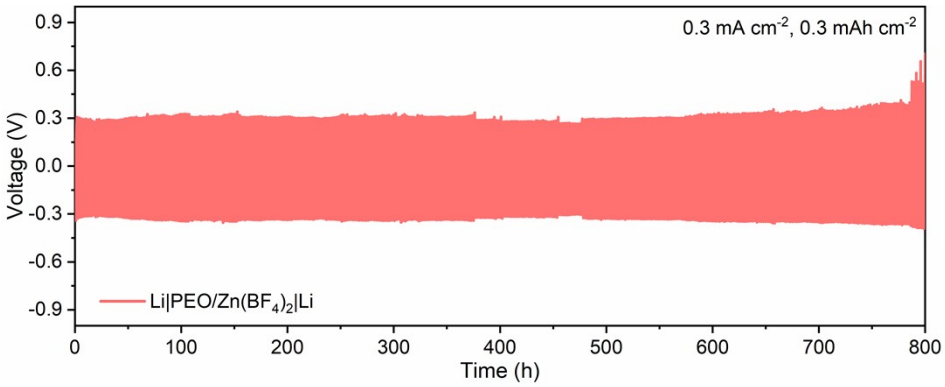

Fig. S7 Voltage profile of the Li|PEO/$Zn(BF_4)_2$|Li symmetric cell at 0.3 mA cm^{-2} with an areal capacity of 0.3 mAh cm^{-2}.

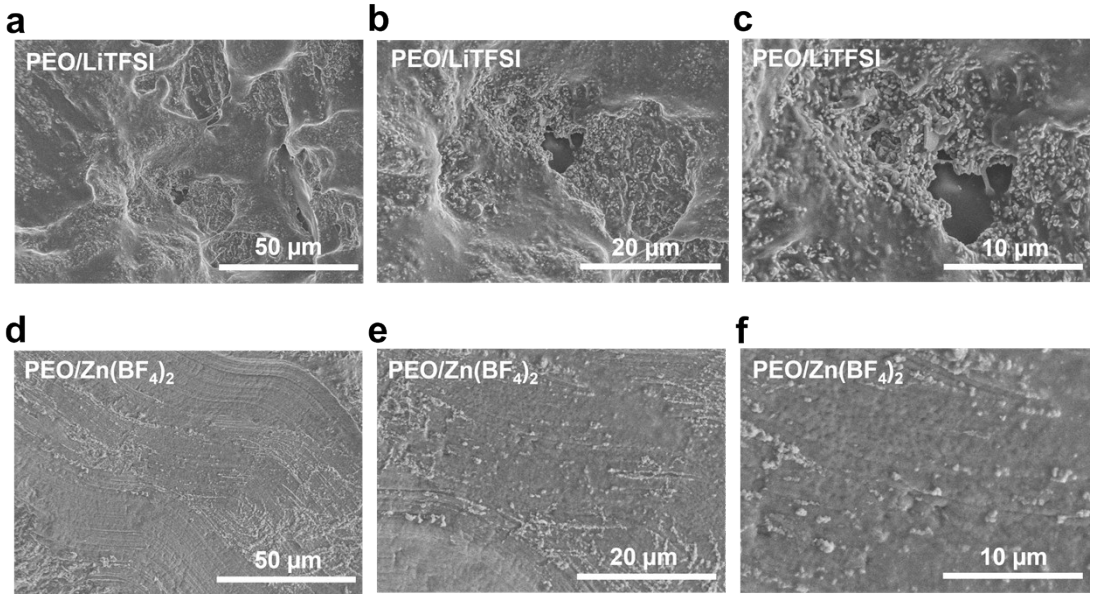

Fig. S8 Surface SEM images of the cycled Li anodes retrieved from the cycled Li||Li cells in (a,b,c) PEO/LiTSFI and (d,e,f) PEO/$Zn(BF_4)_2$.

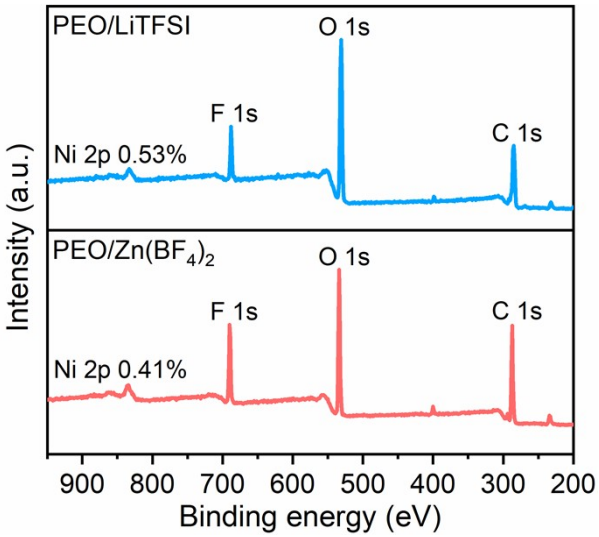

Fig. S9 XPS survey spectra of cycled Li anodes in Li||NCM811 cells with PEO/$Zn(BF_4)_2$ and PEO/LiTFSI.

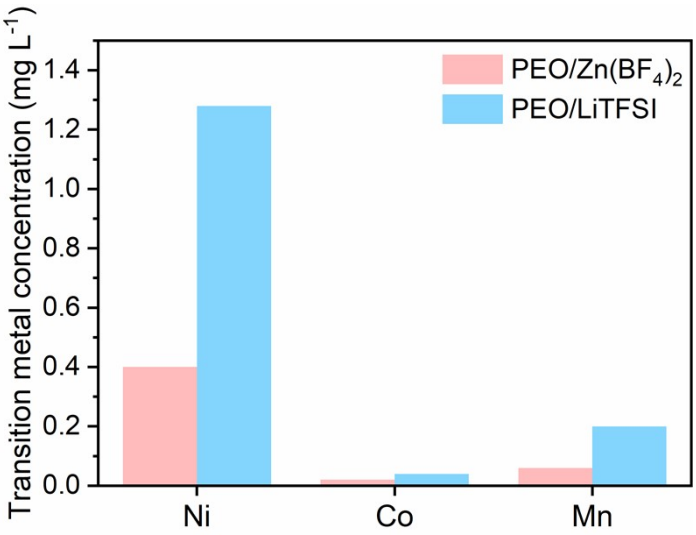

Fig. S10 Transition metal residuals on the Li anodes detected by ICP-OES.

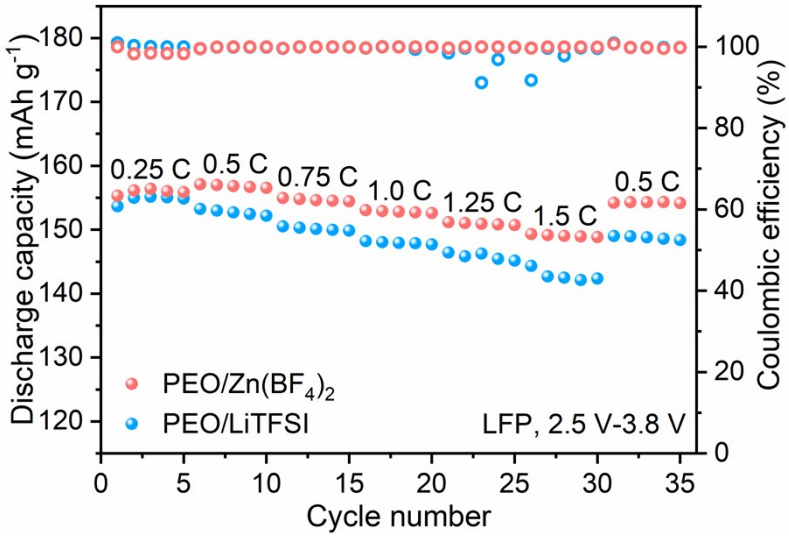

Fig. S11 Rate performance of the Li||LFP cells with different electrolytes.

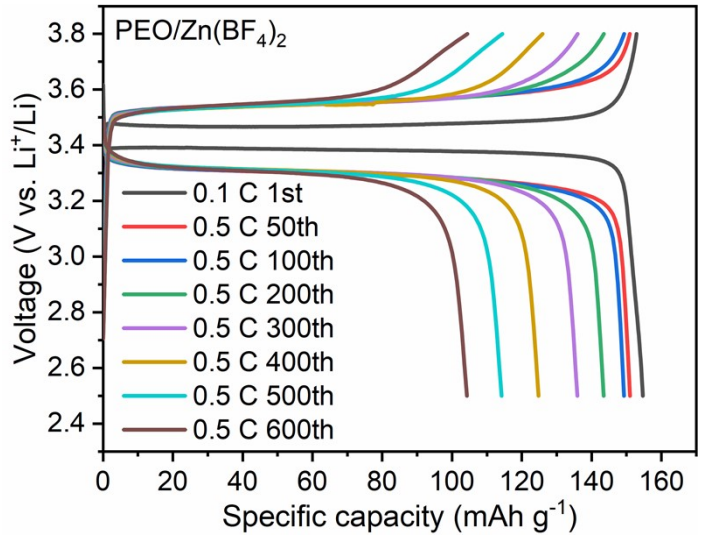

Fig. S12 Galvanostatic charge/discharge voltage profiles of the Li|PEO/$Zn(BF_4)_2$|LFP cells in different cycles.

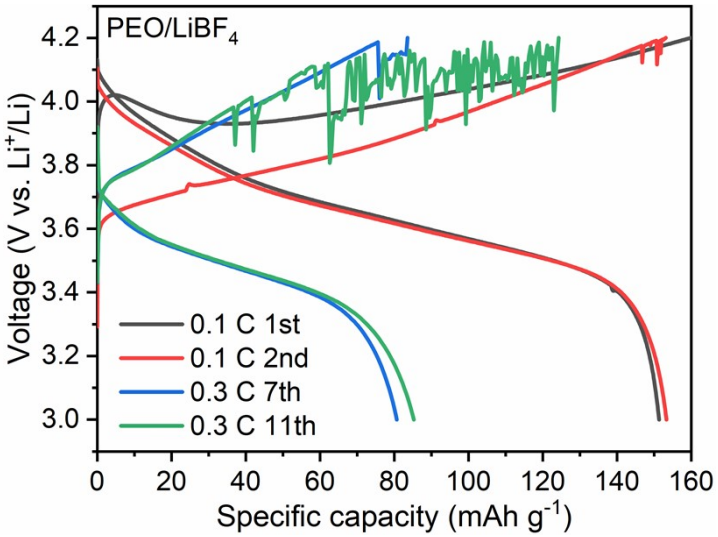

Fig. S13 Galvanostatic charge/discharge voltage profiles of the Li||NCM811 cells with $PEO/LiBF_4$.

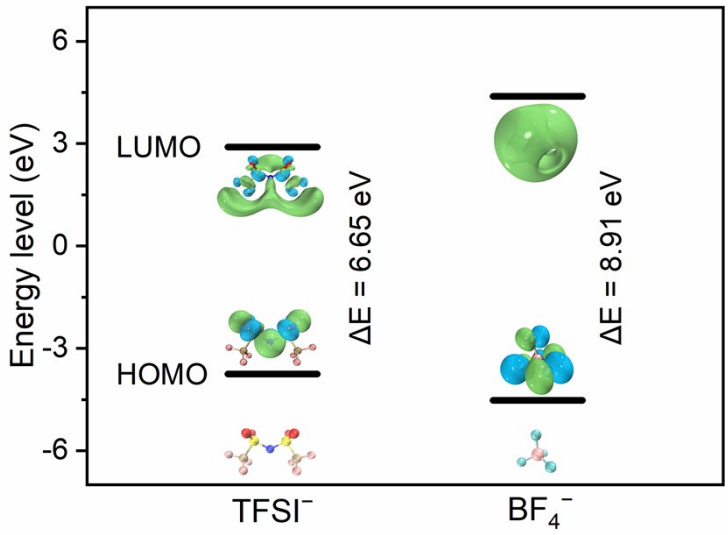

Fig. S14 HOMO and LUMO energy levels of $TFSI^-$ and BF_4^-.

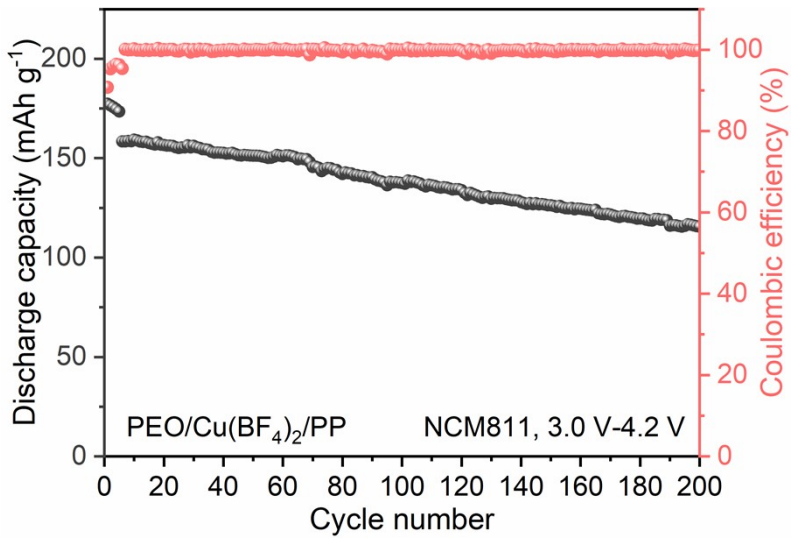

Fig. S15 Cycling performance of the Li|PEO/$Cu(BF_4)_2$/PP|NCM811 cells.

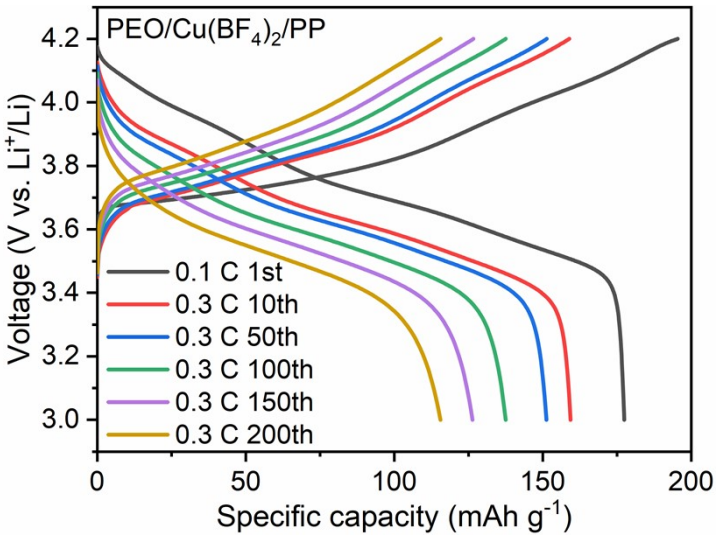

Fig. S16 Galvanostatic charge/discharge voltage profiles of the Li|PEO/$Cu(BF_4)_2$/PP|NCM811 cells in the different cycles.

Table S1. Ionic conductivities and the corresponding E_a values for PEO/LiTFSI.

Solid polymer electrolyte	Temperature (℃)	Ionic conductivity (S cm^{-1})	ΔE_a (eV)
PEO/LiTFSI	25	8.34×10^{-6}	
	30	1.43×10^{-5}	0.38
	40	4.34×10^{-5}	
	50	9.04×10^{-5}	
	60	1.54×10^{-4}	0.22
	70	2.58×10^{-4}	

Table S2. Ionic conductivities and the corresponding E_a values for PEO/$Zn(BF_4)_2$.

Solid polymer electrolyte	Temperature (℃)	Ionic conductivity (S cm^{-1})	ΔE_a (eV)
PEO/$Zn(BF_4)_2$	25	3.94×10^{-5}	
	30	5.85×10^{-5}	0.28
	40	1.36×10^{-4}	
	50	2.77×10^{-4}	
	60	3.98×10^{-4}	0.15
	70	5.83×10^{-4}	

Table S3. Thermal property data of SPEs obtained from DSC.

Solid polymer electrolyte	T_g (℃)	T_m (℃)	ΔH_m (J g^{-1})	X_c (%)
PEO/LiTFSI	−46.9	39.4	32.3	25.8
PEO/$Zn(BF_4)_2$	−52.3	40.0	26.3	20.6